Humidification–dehumidification desalination process using green hydrogen and heat recovery

ENVIRONMENTAL RESEARCH
INFRASTRUCTURE AND SUSTAINABILITY

OPEN ACCESS

RECEIVED
22 September 2021

REVISED
17 November 2021

ACCEPTED FOR PUBLICATION
23 November 2021

PUBLISHED
20 December 2021

PAPER

Humidification–dehumidification desalination process using green hydrogen and heat recovery

A Brunini[1,2,*], M C García[1], A A Melgarejo[3] and R G Rodríguez[1]

[1] Instituto de Tecnología Aplicada, Unidad Académica Caleta Olivia, Universidad Nacional de la Patagonia Austral, Ruta 3 Acceso Norte, Argentina
[2] Consejo Nacional de Investigaciones Científicas y Técnicas, Godoy Cruz 2290 (C1425FQB) CABA, Argentina
[3] Facultad de Ingenieria, Universidad Nacional de La Plata, Calle 1 y 47—La Plata (B1900TAG)—Buenos Aires, Argentina
[*] Author to whom any correspondence should be addressed.

E-mail: abrunini@yahoo.com.ar

Keywords: desalination, humidification–dehumidification, hydrogen

Supplementary material for this article is available online

Abstract

We propose the use of green hydrogen as fuel for a seawater heater in a humidification/dehumidification (HDH) desalination plant to increase its productivity, to allow scaling to large dimensions without negative environmental effects, and to guarantee continuous operation. We develop a mathematical model of the proposed HDH configuration. For operating conditions that guarantee very low NO_x production, the fuel consumption is ∼0.03 kg of H_2 per kg of pure water produced. If the exhaust gases from the seawater heater are used for heat recovery, the GOR of the equipment may increase by up to 39% in relation to the same equipment operating without heat recovery. The operation cost of freshwater is comparable to the costs obtained by other equipment in the literature. If the water produced in the combustion of hydrogen is condensed during the heat recovery process and then added to the freshwater produced, the production cost is reduced by 20%. We found that an excess of air in the air + fuel mix beyond the minimum value appropriate for a low NO_x generation does not provide significant benefits. The efficiency of the seawater heater has an impact on the production of pure water, but this impact is strongly mitigated by the heat recovery process. Fuel consumption increases proportionally with the decrease in the effectiveness of the heat recovery device, which is a key parameter for optimal performance. A hydrogen heater is also a good alternative as an auxiliary power source to guarantee continuous operation. In sunny hours a H_2 heater may be used to increase productivity preheating the seawater, and at night the system could operate 100% based on H_2.

1. Introduction

Large-scale desalination plants are based on membrane filtration or thermal distillation. Large amounts of fossil fuel are consumed for the operation of these plants, either directly or indirectly, releasing greenhouse gases and contributing to the global warming of the planet [1]. One possible strategy to mitigate this problem is to use clean energy sources [2] like solar radiation.

Solar stills, which have long been used to produce drinking water on a small scale, use solar radiation to evaporate water without boiling, and then it does not produce greenhouse gases. Within a solar still, the circulating air carries humidity, which is further condensed in a cooler region of the equipment, releasing the enthalpy of condensation, which is lost to the environment. The thermal efficiency of solar stills is very limited, not superseding 30%–40% [3] because the energy from the condensation of water cannot be recovered. This is due to the design of the equipment itself: in solar stills, the condensation surface is also the transparent cover through which the solar radiation enters to the system. For this reason, scaling up solar stills to plants with large productions of drinking water is unfeasible.

In humidification/dehumidification (HDH) air is usually used as the carrying gas, but in contrast to solar stills, the evaporator, condenser, and water heater are separated parts of the equipment and can be designed to maximize the recovery of the enthalpy of condensation of humid air [1, 4]. Due to this reason, theoretical and experimental studies of the desalination process by HDH technology is steadily gaining increasing interest.

Up to the present, only small-scale HDH plants, essentially experimental in nature, have been designed, assembled, and tested. Most investigations have focused their attention on the search for configurations that maximize performance. The main disadvantage of the solar HDH systems is their low productivity. The scaling to large production of freshwater maintaining a low environmental impact remains unsolved [5, 6]. This is because the scale of solar-powered HDH plants is limited by the surface of the solar collector, which represents near 35% of the total costs of the equipment. Additionally, the surface of a solar collector for a medium-scale HDH plant is prohibitively large. Besides, in regions with freshwater scarcity and limited solar radiance, HDH cannot operate with a solar collector as the energy source. The use of water heaters using fossil fuels would degrade one of the greatest virtues of HDH, impacting negatively on the environment. This problem could be superseded if geothermal energy were accessible, but this is not the case in many regions around the Earth. In these regions, the implementation of HDH as a viable technology to supply freshwater would require the use of an alternative heating source. In [7] it is shown that the water temperature plays an important role in the productivity of the freshwater and that an extra heat source, when available, should be located immediately before or after the solar collector. Additional energy sources are also mandatory to guarantee a continuous operation.

Preheating of seawater using hot flue gases was analyzed previously [8–10], but considering flue gases from the combustion of fossil fuels. At present, most countries, and especially the European Union, are making great efforts to move to a greenhouse-free economy. To achieve its goal of becoming climate neutral by 2050, the EU plan is to install 40 GW of renewable energy to feed hydrogen electrolyzers in the next decade [11]. For this reason, the development of technologies for the use of hydrogen as fuel for steam boilers has recently taken a strong boost, especially due to the impact that its application to home heating would have [12]. The use of hydrogen as substitute energy for natural gas for steam boilers would allow to save energy costs [13]. On the other hand, the by-products of the complete combustion of hydrogen (neglecting secondary reactions) are pure water in the form of steam [14] and other gases already present in the air if it is used as the oxidant. Therefore burning green hydrogen may be considered a 'clean' source of energy [15]. Green hydrogen generated by electrolysis an the use of fuel cells were proposed along with reverse osmosis desalination plants, to have a backup of power when the demand increases [2, 16]. So far, green hydrogen has not been proposed as a power source for thermal desalination technologies. In desalination equipment based on HDH technology, a seawater heater using green hydrogen as fuel would have some remarkable advantages because it has the highest energy content of any common fuel by weight and it is more efficient than many other energy sources, including some renewable alternatives.

In this work we present for the first time a water desalination equipment with HDH technology which uses hydrogen to heat seawater. We will propose a possible configuration that takes advantage of the exhaust gases from the water heater and reduces the cost of fresh water production. We will build a mathematical model of the equipment, which includes, for the first time, a thermodynamic analysis of energy recovery of the exhaust gases from a boiler that uses hydrogen as fuel. With this model, we will carry out a study of the operating conditions of the proposed equipment and we will analyse the viability of scaling the HDH technology to a high productivity installation, without causing the generation of nitrogen oxides in the combustion process. Finally, we will analyse some relevant issues in relation to the sustainability of this proposed technology, some of its limitations and questions that would be worth studying in the future.

2. A basic HDH desalination equipment

A basic HDH desalination equipment configuration is shown in figure 1. The HDH cycle is as follows: the saline water enters the condenser at a temperature T_1. The water circulates through the condenser to condensate partially the water vapor from the air leaving the humidifier at the temperature T_9. The latent heat of condensation of water rises the seawater temperature, leaving the condenser at the temperature T_2, whereas the air which loses most of its humidity is cooled to the temperature T_6. It enters the humidifier, repeating a closed cycle. At the outlet of the condenser, the water enters a seawater heater, whose nature does not need to be specified at this moment. The water leaves the heater at the temperature T_4, to be sprayed into the humidifier for the purpose of bringing it into contact with the air stream which is humidified.

In what follows, we will develop a mathematical model of this equipment with a set of mass and energy balance equations. The following assumptions are made:

(a) The system is operated at a steady-state.

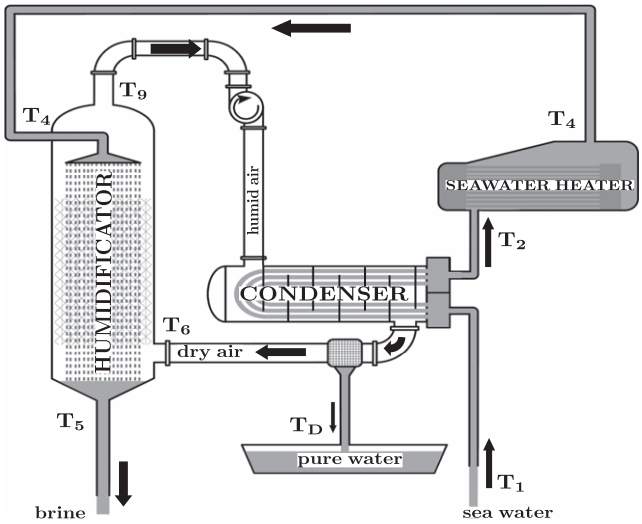

Figure 1. HDH equipment closed in air and open in water.

(b) The potential and kinetic energy terms are negligible.
(c) The system works at atmospheric pressure.
(d) The salinity of the water is typical of seawater (35 g kg^{-1}).
(e) The pump and blower powers ($\sim$ 0.03 kWh^{-1} per m^3 of freshwater produced [17, 18]) are negligible compared with the water heater power.

For the thermophysical properties of seawater we used the correlations provided by [19].

2.1. Humidifier

According to figure 1, the energy balance of the humidifier is [20]

$$\dot{m}_a h_{a,6} + \dot{m}_w h_{w,4} = \dot{m}_a h_{a,9} + \dot{m}_B h_{w,5} + \dot{Q}_{H,loss}, \tag{1}$$

where $\dot{Q}_{H,loss}$ is the heat loss to the environment through the humidifier isolation. We will assume that for dry air at $T_{ref,a} = 0°C$, the reference value for the enthalpy is $H_0 = 0$. Therefore, the enthalpy of humid air at temperature T_j is written as [21]

$$h_{a,j} = Cp_a T_j + x(T_j)(Cp_v T_j + \lambda). \tag{2}$$

The latent heat of evaporation of water λ and the sensible heats of air Cp_a, water vapor Cp_v, and liquid water Cp_w are considered constants. The absolute humidity of the air is obtained in terms of the atmospheric pressure P and the vapor pressure of saturation P_v at the dry bulb temperature, using the expression given by [22] (see supplementary material (https://stacks.iop.org/ERIS/1/035005/mmedia)). We also introduced the relative humidity of air $H_{R,j} (0 < H_{R,j} \leqslant 100\%)$ because the air may not be saturated at points $j = 9$ although at point $j = 6$ the air is probably saturated, because it just came from a condensation process [23]. Therefore

$$x(T_j) = 0.621\,98 \frac{(H_{R,j}/100) P_v(T_j)}{P - (H_{R,j}/100) P_v(T_j)}. \tag{3}$$

For most HDH equipment P is the atmospheric pressure, and we will assume this working condition for our installation. To complete the humidifier model we will use its effectiveness. The effectiveness is the actual change of enthalpy rate produced in relation to the maximum change in total enthalpy rate that can be achieved [24], and it is computed as

$$\epsilon_H = \max \left\{ \frac{\dot{H}_{wo} - \dot{H}_{wi}}{\dot{H}_{wo}^{ideal} - \dot{H}_{wi}}, \frac{\dot{H}_{ai} - \dot{H}_{ao}}{\dot{H}_{ai} - \dot{H}_{ao}^{ideal}} \right\}, \tag{4}$$

where $\dot{H} = \dot{m}h$ (water or air as appropriate) and we have used sub-indices i for inlet values, o for outlet values, a for air and w for water. In this expression H_{wo}^{ideal} is the enthalpy of water at the dry air inlet temperature, and H_{ao}^{ideal} is the enthalpy of saturated air at the water inlet temperature.

The mass balance in the humidifier is expressed as

$$\dot{m}_{\mathrm{B}} = \dot{m}_w - \dot{m}_{\mathrm{a}}[x(T_9) - x(T_6)] = \dot{m}_w - \dot{m}_{\mathrm{p}w} \tag{5}$$

where $\dot{m}_{\mathrm{B}}$ is the mass flow rate of brine leaving the humidifier at point (e). The mass flow of air $\dot{m}_{\mathrm{a}}$ is constant.

2.2. Condenser

As the air stream flows in a closed loop, the balance of enthalpy of the air in the condenser is the same as for the humidifier. We then have [21]

$$\dot{m}_w h_{w,1} + \dot{m}_{\mathrm{a}} h_{\mathrm{a},9} = \dot{m}_w h_{w,2} + \dot{m}_{\mathrm{a},6} + \dot{m}_{\mathrm{p}w} h_{w,6} + \dot{Q}_{\mathrm{C,loss}}. \tag{6}$$

We have assumed that the distillate water leaves the condenser at the same temperature of the air stream T_6.

As for the humidifier, we also define the condenser effectiveness as

$$\epsilon_{\mathrm{C}} = \max\left\{\frac{\dot{H}_{w\mathrm{o}} - \dot{H}_{w\mathrm{i}}}{\dot{H}^{\mathrm{ideal}}_{w\mathrm{o}} - \dot{H}_{w\mathrm{i}}}, \frac{\dot{H}_{\mathrm{ai}} - \dot{H}_{\mathrm{ao}}}{\dot{H}_{\mathrm{ai}} - \dot{H}^{\mathrm{ideal}}_{\mathrm{ao}}}\right\}. \tag{7}$$

The mass balance in de condenser is

$$\dot{m}_{\mathrm{p}w} = \dot{m}_{\mathrm{a}}[x(T_9) - x(T_6)]. \tag{8}$$

The mass flows of air $\dot{m}_{\mathrm{a}}$ and sea water $\dot{m}_w$ are constant.

2.3. Sea water heater

The energy balance in the sea water heater is given by

$$\dot{Q} = \dot{m}_w C p_w (T_4 - T_2) \tag{9}$$

where $\dot{Q}$; is the rate of effective heat absorbed by the feed water and it is known [21]. In this case we do not consider heat exchange with the environment.

With this last expression we completed the thermodynamical model of the HDH equipment. The temperature of the feed water, the mass flow rates of water and the mass flow rate of air are considered known quantities. There are five unknown temperatures: T_2, T_4, T_5, T_6, and T_9, and five equations: (1), (4), (6), (7) and (9). The pure water mass flow rate and the brine mass outflow rate can be obtained as a function of the temperatures and relative humidities by (3) and (5). This equations have been extensively used to model basic HDH equipments. Nevertheless, we have validated the model using the experimental data furnished by [21], and details of the procedure and results can be found in the supplementary material. The experimental results of [21] could be adequately reproduced, and we concluded that the thermodynamical model works properly.

3. Using H_2 in a HDH desalination plant

A heat source that increases the temperature of the water in the humidifier would allow to increase the productivity of the equipment [7]. It would also allow a scaling up to higher productions. As discussed before, the use of fossil fuels is not an alternative given the negative environmental impact. In this section we will analyse the use of hydrogen as an energy source to heat the seawater. A thermodynamical model of the H_2 sea water heater is developed in the next subsections.

3.1. H_2 + air seawater heater

The development of H_2 boilers is just now taking a strong impulse, but up to the present, a thermodynamic analysis of these devices, nor data of their operation have been published. For this reason we warn readers that it is not possible to compare all our results with published or experimental data.

3.1.1. Temperature of the flame

The by-products and the temperature of combustion in the burner of the seawater heater depend on the fuel and oxidant used. In this study, we will consider H_2 as the fuel, and air as the oxidant. As this is the first analysis of the use of H_2 as fuel in an HDH plant, we will introduce some simplifying assumptions:

- (i) The air humidity in the H_2 − air mix is negligible.
- (ii) We do not consider other constituent gases of air beyond oxygen and nitrogen.
- (iii) The mix is made at the standard temperature ($T^{\oplus} = 25°\mathrm{C}$).
- (iv) The combustion is complete.

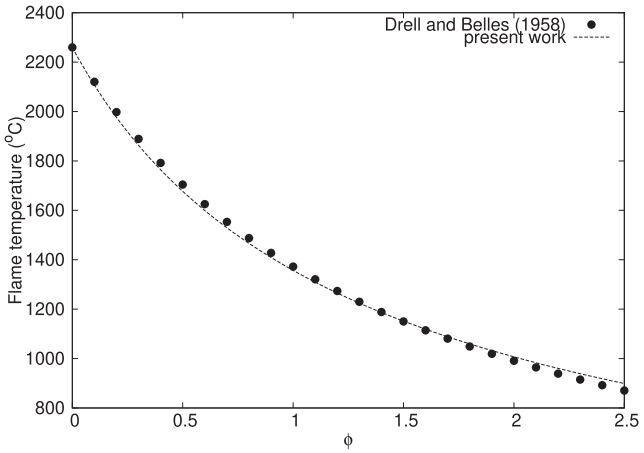

Figure 2. Temperature of combustion of H_2 + air vs the excess of air in the mix given by (10), with $Lc = 118.680 \times 10^6$ J kg^{-1} and dry air at the standard temperature (see main text). The temperature computed by [26] is also shown.

• (v) Molecular dissociations of flue gases are no considered.

Taking into account these factors would produce minor changes in the results. In these conditions the temperature of combustion $T_{\rm COMB}$ is obtained by solving the equation [25]

$$Lc = \int_{T^{\oplus}}^{T_{\rm COMB}} [8.995 Cp_v + 26.35 Cp_{\rm N_2} + 34.4\phi Cp_{\rm a}]{\rm d}T, \tag{10}$$

where $Lc = 118.680 \times 10^6$ J kg^{-1} is the lower heating value of H_2, and

$$\phi = \frac{\dot{m}_{\rm air} - \dot{m}_{\rm air_{ST}}}{\dot{m}_{\rm air_{ST}}}, \tag{11}$$

is the excess of air mass flow rate in the mixture respect to the air needed for a stoichiometric mix. Appropriate correlations for the specific heat capacities where used, and they can be found in the supplementary material. In figure 2 we show the temperature of combustion of H_2 given by (10) as a function of the excess of air in the H_2 − air mixture.

It is important to note that the flame temperature should remain below ∼1350 °C in order to inhibit, or maintain very low, the production of NO_x gases [27]. Nitrogen oxides have negative consequences for human health, cause acid rain, and also contribute to the global warming. Therefore, $\phi > 1.2$–1.3 guarantees low NO_x production [28] and we will test the equipment under this restriction.

3.1.2. Exhaust gases

The complete combustion of a given mass rate $\dot{m}_{\rm H_2}$ of hydrogen using air as the oxidant will produce

$$H_2 + 34.4(1+\phi){\rm air} \Rightarrow 8.995 H_2O + 26.35 N_2 + 34.4\phi{\rm air}, \tag{12}$$

of exhaust gases (H_2O in the form of steam).

The seawater heater efficiency $\epsilon_{\rm B}$ is defined as the fraction of the total heat produced that is absorbed by the water to raise its temperature to the desired value [29]. In this paper we will use the expression

$$\epsilon_{\rm B} = \frac{\dot{m}_w Cp_w (T_4 - T_3)}{\dot{m}_{\rm H_2}(Lc + 8.995\lambda)}. \tag{13}$$

Typical water heater efficiencies range between 0.8 and 0.9 [29]. The exhaust gases are the main source of heat losses. The temperature of the exhaust gases may be computed by means of the empirical expression [30–32]

$$T_7 = T_{\rm COMB}(0.98 - \epsilon_{\rm B})^{1/1.128}, \tag{14}$$

which considers 2% of heat lost to the environment by radiation and convection [32]. In this paper, we will not take into account losses due to incomplete combustion, production of ashes and slag. We want to remark that this expression was obtained for gas fuels other than H_2. Changing a heater from fuel gas to H_2 fuel results in a mass flow reduction through the heater that could impact the convective heat transfer to the water and thus the stack temperature, with the consequent variation of the exponent in (14). Very few information is about

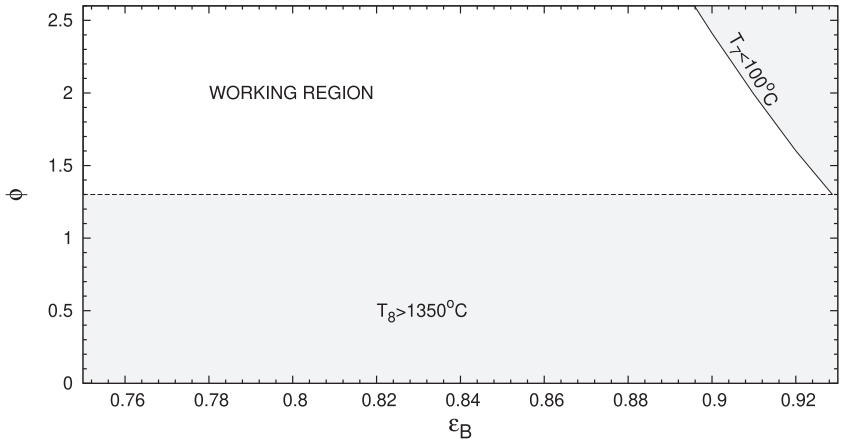

Figure 3. In the white region the temperature of the exhaust gases are below the region of NO_x production and simultaneously above the water vapor dew point temperature.

this question (there is not an expression like (14) for H_2 in the literature), but it seems that stack temperature does not change substantially when switching from natural gas to H_2 [33]. The heater efficiency should also change very little [33]. The minimum acceptable exhaust gas temperature for heaters and boilers is usually 120 to 130°C in order to avoid condensation. In our investigation, we will impose the condition $T_7 > 100°C$. This is a rather low value in relation to the standards considered for water heater operations but nevertheless ensures us that we cover all possible conditions of operation without losing generality and remaining above the dew point temperature of water vapor at atmospheric pressure. Within the imposed conditions, the working region of the seawater heater is shown in figure 3.

There is a maximum efficiency for the seawater heater of $\epsilon_B \sim 93\%$ because above this maximum efficiency the conditions we have imposed for the flame temperature and for the temperature of the exhaust gases cannot be fulfilled simultaneously: according to (14), if the flame temperature is $T_{COMB} < 1350°C$, the condition to have $T_7 \geqslant 100°C$ is

$$\epsilon_B \leqslant 0.98\left(\frac{100\ °C}{1350\ °C}\right)^{1.128} \simeq 0.927. \tag{15}$$

The sea water heater efficiency also depends on the excess of air used in the mix, but this effect was not considered in this study.

3.2. Effect of the water temperature in the pure water flow rate

We are now in a position to calculate the effect of increasing the water temperature on the production of pure water. As pointed out by [7], the rate of pure water production increases very significantly with an increase in the humidifier water inlet temperature (it is expected because of the exponential increase in the absolute humidity of the saturated air with temperature). Pure water mass flow rate vs the temperature of water at the humidifier inlet is shown in figure 4 where we used the parameters of the equipment (ϵ_C, ϵ_h, $\dot{Q}_{C,loss}$, $\dot{Q}_{H,loss}$ and $H_{R,9}$) already computed in the supplementary material section but varying T_4.

As it was already shown by [7], the relation between T_4 and $\dot{m}_{pw}$ is basically linear. In our case the growth rate on pure water production is of 0.057 kg h^{-1} for each degree that the water temperature increases. For this reason, to increase the productivity of HDH technology, an additional energy source to solar energy is necessary.

3.3. Heat recovery

The use of fuel, either liquid or gaseous, to heat the seawater will generate heat losses through the exhaust gases, which on the other hand, are the most important losses in the process. It is essential to add some device to recover part of it. The alternative configuration we will consider to evaluate the use of H_2 in HDH desalination with heat recovery is shown in figure 5.

The configuration of the desalination cycle is the same as before, corresponding to an open cycle for the water flow and a closed cycle for the air stream. Now, the water leaves the condenser at the temperature T_3, whereas the exhaust gases that leave the seawater heater at the temperature T_7 exit the heat exchanger that is used as a recuperator at the temperature T_8.

The thermodynamical model for the humidifier and the condenser is exactly the same as before (equations (1), (4), (6) and (7)), and they will not be shown here again.

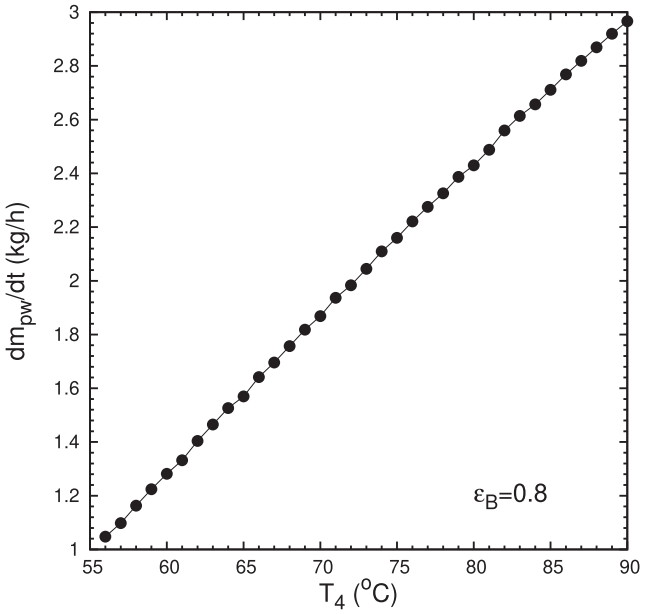

Figure 4. Pure water mass flow rate vs the temperature of water at the humidifier inlet.

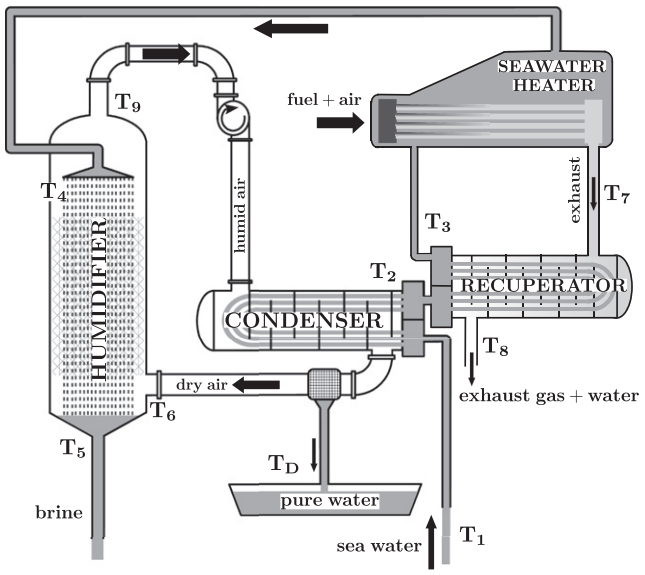

Figure 5. HDH equipment with a H_2 + air heater and recuperation of flue gases.

Let us consider that the exhaust gases that come out of the stack of the seawater heater are composed of water vapor and N non-condensable gases (in this case $N = 2$, the excess of air used and nitrogen). We will assume that

(a) The flue gases are at a temperature high enough to guarantee that the water does not condense before entering to the recuperator.

(b) The water vapor of the flue gases is completely condensed inside the recuperator.

(c) There are not heat exchange with the environment.

Condition (b) is fulfilled if the exit temperature of the flue gases is below the dew point. The dew point can be computed using Dalton's law for the vapor partial pressure [34]. Full details are given in the supplementary material, but it is below 100°C. Under these conditions the enthalpy balance of the recuperator is given by

$$\dot{m}_w^{\mathrm{E}}[h_w^{\mathrm{E}}(8) - h_w^{\mathrm{E}}(7)] + \sum_{i=1}^{N} \dot{m}_{g_i}[h_{g_i}(8) - h_{g_i}(7)] + \dot{m}_w[h_w(3) - h_w(2)] = 0, \tag{16}$$

where we used i for inlet values, o for outlet values, and g for the exhaust gases. The mass flow rate of each species (water vapor, nitrogen and oxygen) is given by (12). To complete the recuperator thermodynamical model, its effectiveness is defined in the same way as for the humidifier and the condenser [24] as

$$\epsilon_{\mathrm{Rec}} = \max\left\{\frac{\dot{H}_{w\mathrm{o}} - \dot{H}_{w\mathrm{i}}}{\dot{H}_{w\mathrm{o}}^{\mathrm{ideal}} - \dot{H}_{w\mathrm{i}}}, \frac{\dot{H}_{\mathrm{gi}} - \dot{H}_{\mathrm{go}}}{\dot{H}_{\mathrm{gi}} - \dot{H}_{\mathrm{go}}^{\mathrm{ideal}}}\right\}. \tag{17}$$

In this expression, $H_{w\mathrm{o}}^{\mathrm{ideal}}$ is the enthalpy of water at the exhaust gases inlet temperature, and $H_{\mathrm{go}}^{\mathrm{ideal}}$ is the enthalpy of the exhaust gases (including condensed water) at the water inlet temperature.

4. Method

In the previous sections, we have shown the set of equations governing the steady-state operation of the HDH equipment. To solve the model we used the following strategy: the whole HDH system is separated into two sub-systems:

(a) A basic HDH subsystem composed of the humidifier and the condenser.
(b) A second subsystem composed of the seawater heater and the recuperator.

The second subsystem provides a mass flow rate of water $\dot{m}_w$ to the humidifier at the temperature T_4. We adopt as the reference for the working parameters of the basic HDH subsystem those provided by the 8 valid experimental runs of [21]. Therefore, the quantities T_2, T_4, $\dot{m}_w$ and $\dot{m}_{\mathrm{p}w}$ are assumed to be known.

Equations (10), (13), (14), (16) and (17) form the governing equations to be solved in order to obtain T_3, T_7, T_8, the mass flow rate of H_2 consumed in the seawater heater, and the mass flow rate of each species of the exhaust gases. (12) is also used to compute the mass of each species of the exhaust gases. In addition, we leave as free parameters the excess of air ϕ, the efficiency of the heater ϵ_{B} and the effectiveness of the recuperator ϵ_{Rec}. As it was already mentioned, we restrict the domain of excess of air to values that guarantee that the temperature of the exhaust gases exceeds 100°C, and on the other hand to values of $\phi \geqslant 1.3$, so that the production of NO_x gases is inhibited or very low. For the recuperator effectiveness we explored values in the range 0.7–0.9 [24, 35], and for the seawater heater from 0.80 to 0.92 [29]. The mathematical model is solved in the following way:

(a) For a given value of ϕ, T_{COMB} is computed by means of (10).
(b) With a given value of ϵ_{B}, T_7 is computed from (14).
(c) With this value of T_7 and a given value of ϵ_{Rec}, we compute T_3, T_8 and $\dot{m}_{\mathrm{H}_2}$ (and therefore the mass of all the exhaust gases thorough (12)) by means of an iterative algorithm applied to the non linear system formed by (13), (16) and (17).

We stopped the iteration when the corrections to the unknowns is less than 10^{-6} in absolute value.

4.1. Performance parameters of the system

We will use gained output ratio (GOR) and operating cost parameter (OCP) parameters to assess the performance of the system. They are presented in the following subsections.

4.1.1. Gained output ratio

To characterize the operation of a thermal desalination equipment, the GOR is widely used. It is computed as the ratio of the latent heat of evaporation of the pure water produced, to the heat used to heat the seawater. It represents the amount of heat that could be recovered during the desalination cycle. According to figure 5, we have

$$\mathrm{GOR} = \frac{(\dot{m}_w - \dot{m}_{\mathrm{B}})\lambda}{\dot{m}_w Cp_w (T_4 - T_3)}. \tag{18}$$

In what follows, we will define also GOR_0 as the gained output ratio obtained in the basic equipment, without heat recovery. In this case the water heater inlet temperature is T_2 (see figure 1) so

$$\mathrm{GOR}_0 = \frac{(\dot{m}_w - \dot{m}_{\mathrm{B}})\lambda}{\dot{m}_w Cp_w (T_4 - T_2)}. \tag{19}$$

As an example, for the second experimental run of [21], whose measured values are $T_2 = 40.4$ °C, $T_4 = 56.6$ °C, $\dot{m}_{\mathrm{B}} = 60.1$ kg h^{-1} and $\dot{m}_w = 61.2$ kg h^{-1}, $\mathrm{GOR}_0 \simeq 0.66$.

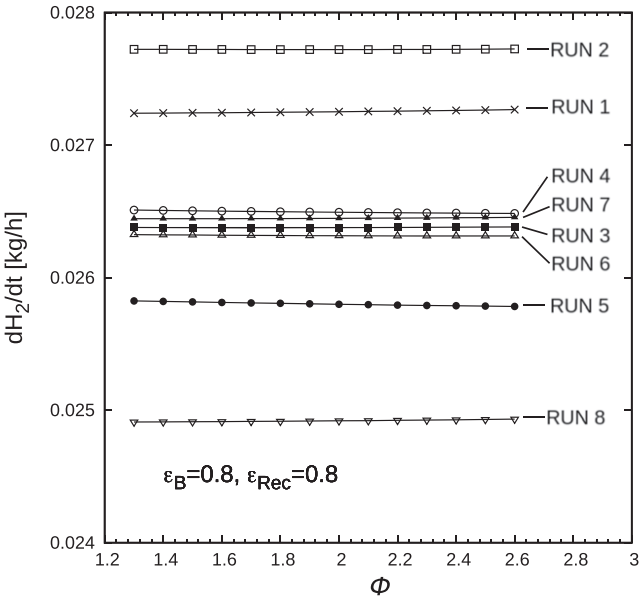

Figure 6. Rate of fuel consumption vs the excess of air ϕ for the parameters of the 8 experimental runs of [21]. We used $\epsilon_{\mathrm{B}} = 0.8$ and $\epsilon_{\mathrm{Rec}} = 0.8$.

4.1.2. Operating cost parameter

OCP gives the cost of the energy consumed to produce 1 kg of freshwater, and it is given by

$$\mathrm{OCP} = \frac{\mathrm{COST}(\mathrm{H}_2) \times \dot{m}_{\mathrm{H}_2}}{\dot{m}_{pw}}. \tag{20}$$

$\mathrm{COST}(\mathrm{H}_2)$ is the unit cost of H_2, and depends on the technology used for its production. One of the most well developed technology for the production of green hydrogen is electrolysis, where electricity produced by renewable sources is used to split water into hydrogen and oxygen. According to recent evaluations [36], green hydrogen is produced at a cost of 4–5 u$s kg^{-1}, and considerable effort is dedicated to reduce this cost to 1 u$s kg^{-1} by 2050. We will use these values in our analysis. Although this indicator considers only the cost of energy to evaluate the cost of water (in this case the cost of the hydrogen used to heat the seawater) we must take into account that it is the most relevant factor in water desalination cost structure. A comprehensive analysis, leading to a more accurate indicator, such as the levelized cost of water, demands the inclusion of the cost of the facilities, their maintenance, operation, amortization of capital, etc. The price of the hydrogen that we are using already considers all these factors, and the cost of the facilities of a HDH plant like the one proposed here would only be possible by making an adequate dimensioning of the equipment, which is beyond the scope of this work. Nevertheless, as an example, specific values of capital cost of an experimental HDH plant are given in [37]. The equipment, maintenance and operation costs of the produced water is about 10% the contribution from the energy cost. In this sense, OCP can be taken as a good indicator of the cost of the fresh water produced.

5. Results

In figure 6 we show the rate of H_2 consumption as a function of the excess of air for the operating conditions of the 8 runs reported in [21].

Although the maximum relative variation in pure water production among all 8 runs is ∼43%, the hydrogen consumption varies only by ∼11%. We see that run 2 and run 8 represent extreme cases. Considering the reported values in [21] (see supplementary material), we see that the heat needed to raise the water temperature from T_2 to T_4 is the maximum and minimum respectively for runs 2 and 8. This is shown in figure 7.

The hydrogen consumption of the complete equipment reflects the behaviour shown if figure 7.

In figure 8 we show the improvement of the GOR when heat recovery is applied. The GOR increases by about 31%–32% with respect to the GOR_0 of the basic equipment.

It is worth noting that GOR and fuel consumption are directly linked. Using (13) and (18) we have

$$\mathrm{GOR} = \frac{(\dot{m}_w - \dot{m}_{\mathrm{B}})\lambda}{\epsilon_{\mathrm{B}}\dot{m}_{\mathrm{H}_2}(Lc + 8.995\lambda)}. \tag{21}$$

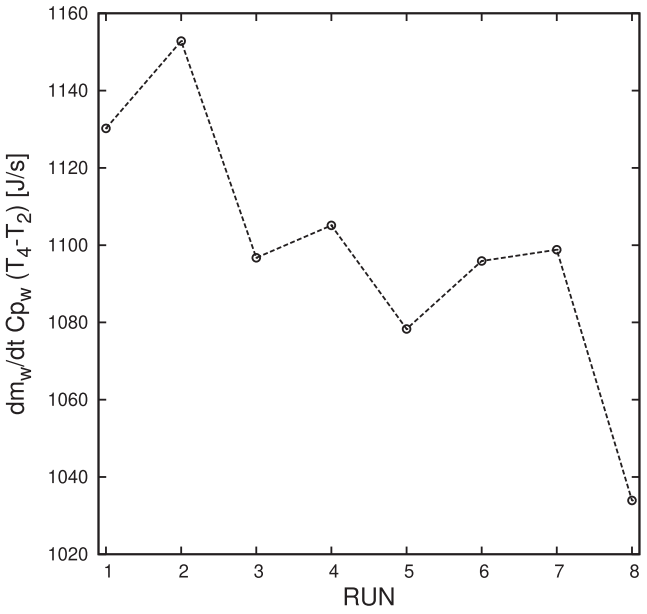

Figure 7. The sensible heat needed to heat the water, for the different runs reported in [21].

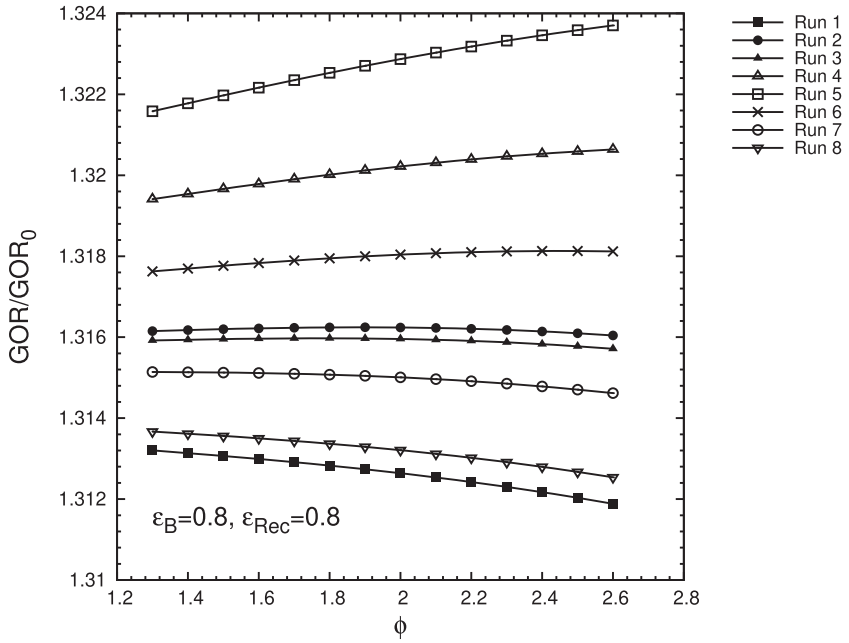

Figure 8. GOR/GOR_0 vs the excess of air used in the mix, for the different runs reported in [21].

In order to analyze the sensitivity to different parameters, we will adopt from here on as reference, run 2 from [21]. The fuel consumption with and without heat recovery is shown in figure 9.

Heat recovery has a deep impact on fuel consumption. The difference is more pronounced for high pure water production, reaching $\sim$24% of fuel savings when $\dot{m}_{pw} \approx 3$ kg h^{-1}.

Regarding the OCP, we have performed two analysis. The OCP vs the efficiency of the seawater heater is shown in figure 10 for the conditions of run 2 [21].

We show the OCP for the present cost of green H_2 and for the cost expected by 2050. We also show for comparison, the OCP of pure water production found by [38]. We observe that heat recovery guarantees that OCP of the proposed equipment falls within the OCP values found by [38]. The mass flow rate of vapor present in the exhaust gases is the same volume of the ultra pure water used in the electrolyzer to produce the amount of hydrogen (without considering losses) burned in the seawater heater. It is $8.995 \times \dot{H}_2$, and according to figure 9, to produce 1 kg of pure water we need $\sim$0.026 kg of H_2. Therefore, for each kg of pure water produced in the HDH cycle, we have also 0.026×8.995 kg of water condensed in the recuperator. Once condensed, this

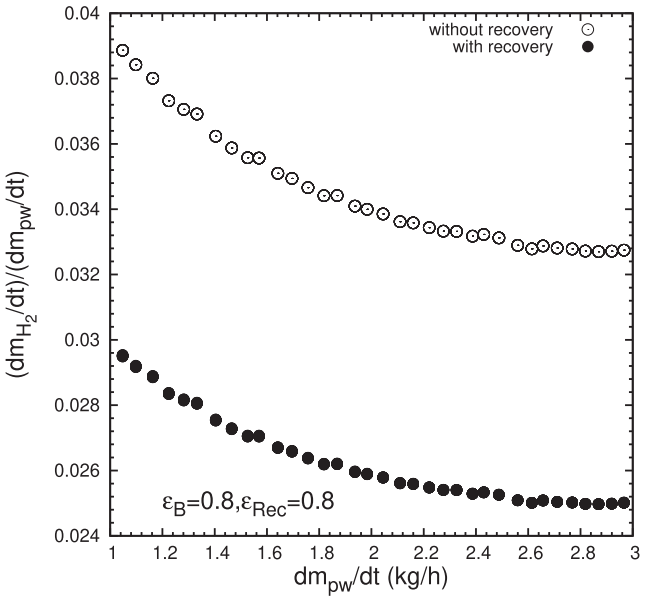

Figure 9. Mass rate of H_2 consumption per kg of pure water produced vs the pure water production rate with and without heat recovery.

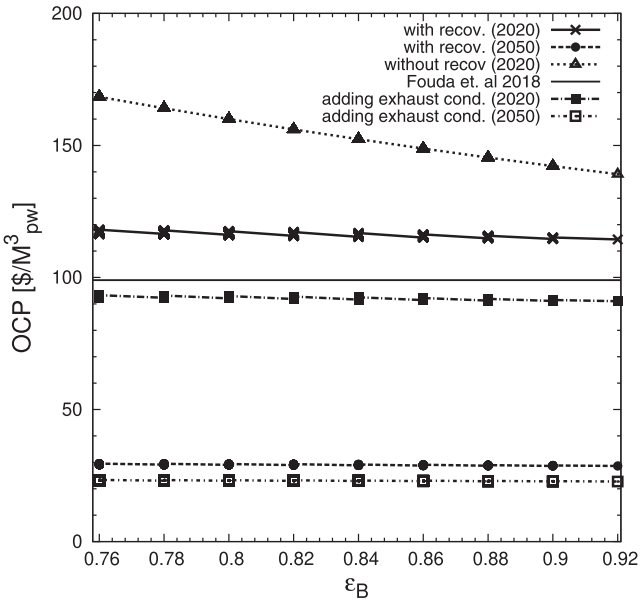

Figure 10. OCP vs the efficiency of the heater.

amount of water can be returned to the electrolyzer or it can be mixed with the pure water produced in the HDH cycle. In this last case we can write

$$\frac{\mathrm{OCP}_{\text{with cond}}}{\mathrm{OCP}_{\text{without cond}}} = \frac{\frac{\text{cost of 0.026 kg of } H_2}{[1+0.026\times 8.995]\ \text{kg of } H_2O}}{\frac{\text{cost of 0.026 kg of } H_2}{1\ \text{kg of } H_2O}} = 0.81. \tag{22}$$

This means that the cost of water is reduced by about 20% if this condensed vapor is added to the fresh water produced in the HDH cycle. If instead this water is returned to the electrolyzer, we can save part of the energy used to produce the ultra-pure water decomposed in the electrolyzer to generate the consumed H_2.

OCP values may be even lower if we consider the fuel savings that occurs when the water temperature rises. This is shown in figure 11.

OCP may be up to 20% lower than the one found by [38]. A 100% efficient electrolyzer could produce 0.03 kg H_2/kWh. Today, depending on the technology used, an electrolyzer has an efficiency of 80%–90%. This means a specific energy consumption of 0.024–0.027 kgH_2/kWh. With our results, we found an equivalent

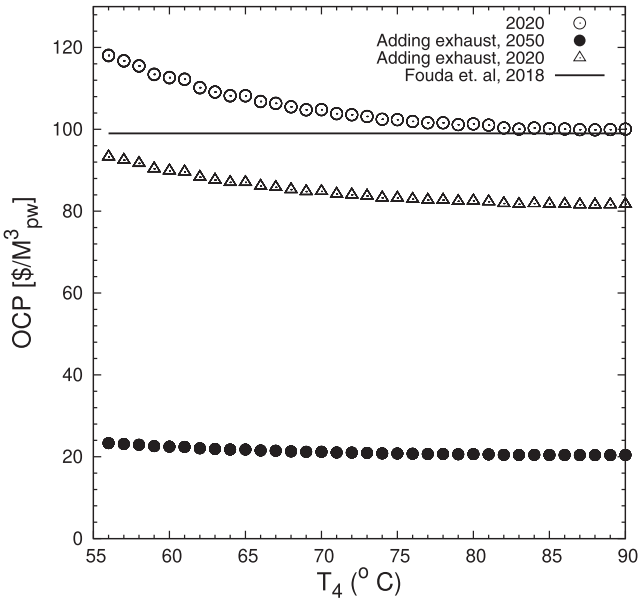

Figure 11. OCP vs the exit temperature of the water from the heater.

Table 1. Comparison with other results reported in the literature.

Energy source	Productivity (kgh^{-1})	GOR	Cost ($ m^{-3})	Reference
Electricity	92.3	—	13.5	[40]
Electricity	71.6	5.38	18	[41]
Electricity	82.1	5.14	—	[42]
Electricity	151.0	5.95	15	[43]
Electricity	50.7	8.12	16	[44]
Electricity	—	0.76	13–18.5	[45]
Electricity	22.3	2.05	51	[46]
Electricity	2.8	2.08	11.4	[47]
Electricity	2.5	0.91	14	[48]
Electricity	12.0	4.07	10.68	[49]
Electricity	8.5	3.911	7.3–34.3	[37]
Electricity	38.8	—	2217–7130	[50]
Electricity & solar	123.7	0.30	99	[38]
Air cond. Waste heat	7.1	1.27	—	[51]
Electricity	1.1	0.66	—	[21]
Waste heat from gas turbine	24 000	—	287	[8]
Natural gas waste heat	15 550	—	1100	[10]
Fuel oil waste heat	20 400	—	1750	[10]
H_2	3	1.04	85.3	Present study[a]

[a]Productivity and cost correspond to the analysed equipment, operating at 90°C and adding the condensed water from the exhaust gases to the fresh water.

mechanical energy consumed in the desalination process of 620–757 kWh m^{-3} of fresh water produced. In addition to working on reducing the cost of hydrogen production, much effort is being made to increase the evaporation in the humidifier. Although we have not considered any specific strategy to do this in the proposed equipment, it would be interesting to mention some of them here:

- Decrease the working pressure inside the humidifier [24]. At atmospheric pressure, saturated air at 75°C carries 0.276 kg kg^{-1} of water vapor, but at half the atmospheric pressure, it becomes saturated with 1 kg kg^{-1}, almost quadrupling productivity and dividing by four the specific energy consumption.
- Multiple extractions of humid air from the dehumidifier and injection to the dehumidifier [39] could improve several times the GOR and the heat recovery of the HDH cycle.

The equipments reported in the literature that do not exclusively use solar energy, make use of electrical energy or waste heat from some heater device to heat the water. In table 1 we compare our results with a series of results reported in the literature.

In table 1 it can be see that the cost of the water produced by our equipment is not very different from those found by other authors.

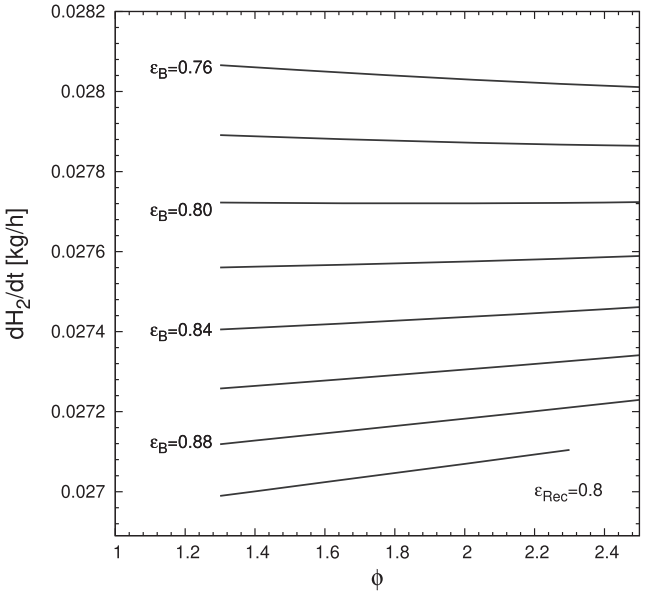

Figure 12. Hydrogen consumption against the excess of air in the mix, for several values of the sea water heater efficiency. T_2, T_4 and $\dot{m}_w$ corresponds to run 2 reported in [21].

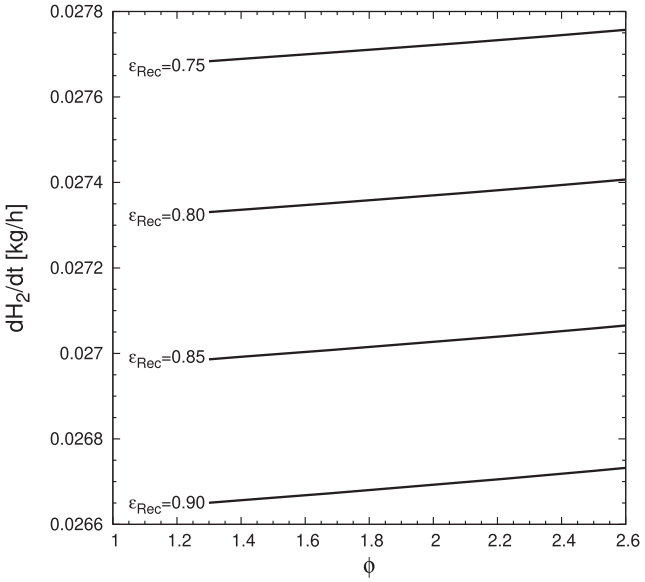

Figure 13. Hydrogen consumption vs the excess of air for different values of ϵ_{Rec}. In this figure, $\epsilon_{\text{B}} = 0.8$.

5.1. Sensitivity to ϵ_{B} and ϵ_{Rec}

In this subsection, we will explore the sensitivity of the results to variations of the efficiency of the seawater heater ϵ_{B} and of the recuperator ϵ_{Rec}. For this analysis, we adopt run 2 from [21] as the reference. In figure 12 we show the variations of the fuel consumption for several values of ϵ_{B}. All these values correspond to a unique value of the recuperator effectiveness $\epsilon_{\text{Rec}} = 0.8$.

As expected, fuel consumption drops with increasing the seawater heater efficiency. However, an increase of 18% in efficiency only impacts 4.5% in fuel saving. The influence of the recuperator effectiveness in the fuel consumption is shown in figure 13.

Fuel consumption increases in direct proportion to the decrease in the efficiency of the recuperator.

6. Conclusions

Since desalination is energy intensive, the use of fossil fuels in thermal desalination plants is not a suitable approach. However, desalination driven by solar energy is only possible for small scale production. Increasing

the productivity of HDH systems requires the supply of additional energy sources. Considering the perspective of environmental sustainability, which is an important issue associated with any desalination processes, we have analysed in this paper the use of a seawater heater burning hydrogen in a HDH desalination equipment.

Among the fuels, hydrogen has the largest calorific value (almost three times that of natural gas). In this sense, our proposal provides an option for increasing the productivity of a HDH desalination plant, either by increasing the temperature of the water if the plant is powered by solar energy, or by serving as the sole source of energy when solar energy is unavailable. We also have developed a thermodynamical model that can be used in the future to evaluate different modifications of the HDH cycle, in order to search for configurations with optimum performance. Our equipment, which is a basic configuration, requires 0.025–0.03 kg of $H-2$ per kg of pure water produced, but this number could be reduced significantly if appropriate techniques are used to increase the rate of evaporation of water in the humidifier, such as mechanical air decompression and/or multiple extractions of vapor. The production costs of pure water are equivalent to those of other HDH equipment reported in the literature. Costs will fall as hydrogen achieves an economy of global scale, which will happen in the next decades.

We found that the use of excess of air in the air + fuel mix beyond the minimum value appropriate for low generation of $NO_x(\phi \sim 1.3)$ does not provide significant benefits in hydrogen consumption regardless of the efficiency values ϵ_{Rec} and ϵ_B (figures 12 and 13). The efficiency of the seawater heater has an impact on the production of pure water, but this is strongly mitigated by the heat recovery process. On the other hand, fuel consumption increases proportionally with the decrease in the effectiveness of the recuperator which is then a key parameter for optimal performance.

Hydrogen is an energy vector carrying water. Burning hydrogen in the HDH process has the advantage that a large fraction of the water that was destroyed in the electrolyzer to produce it is recovered during the desalination cycle. It is especially significant, because desalination is needed in areas where fresh water is limited, and hydrogen production demands large amounts of ultra pure water. If part of this amount of water is recovered during the desalination process, the environmental impact of hydrogen production is reduced.

Beyond the cost, we must not overlook some of the limitations that this technology still has to overcome. The lack of hydrogen pipe networks is one of them. This means that for the moment the hydrogen must be transported or produced where this type of plants are located. Another limitation is the lack of a well developed hydrogen burner technology. This issue is being addressed just now, and it is envisaged that a number of commercial options will be available in the next years.

It is worth to mention that the HDH technology, according to the life cycle analysis carried out by [52], is the one with the lowest environmental impact, which is up to ∼84% less than that of a reverse osmosis plant with similar characteristics. HDH is a technology of low maintenance and extended life time [53], which also reduces its environmental impact.

One of the issues that we have taken into consideration in the design of the HDH cycle, is the emission of greenhouse gases. Hydrogen burning does not produce CO_2 being water, nitrogen and air (if a lean mix is used in the burner) the only constituents of the flue gases. Nevertheless, recombination of nitrogen and oxygen during high temperature burning can cause undesirable production of NO_x. This situation can be adequately controlled by the use of the excess of air in the air–hydrogen mix. We have found that this excess has not a remarkable influence in the equipment performance (see figure 6).

Brine management is another issue of greatest concern in relation to the sustainable management of desalination processes. The large volume of brine produced has economic and environmental implications, especially when it is discharged into sensitive ecosystems. Humidification–dehumidification technology can work with very high salinity [54] allowing recirculation of brine in the dehumidifier. This recirculation reduces the rejected volume of brine. In addition, heat can be recovered from the brine [52] increasing the energetic efficiency and lowering its temperature, which is also another serious environmental problem of thermal desalination processes [55].

Another problem shared by all desalination technologies is the need to add chemicals to the feed water, that are usually washed into the sea after desalination. In thermal processes the use of anti-scalant agents is necessary to prevent the formation of scales within heat exchangers, humidification towers and water heaters. Anti scalants are not necessary if the air is heated instead of the water [56]. Scale formation and corrosion are drastically reduced and so the maintenance costs decrease substantially.

Several questions remains to be investigated. One of them is the sizing of the equipment, which is important for several reasons. On one hand it allows a more accurate evaluation of the cost of water. On the other hand after sizing, we could perform a life cycle analysis of the technology to asses the environmental impact of the desalination process we are proposing. The investigation of other cycles, such as air heating as proposed by [24], is also of relevance and will be addressed in the future. Another question to be investigated is the effect of re-circulation of brine and heat recovery from it, because this would minimize the volume of brine, the cost of operation and the environmental impact.

Acknowledgments

We acknowledge the financial support of the Universidad Nacional de la Patagonia Austral through the Grant PI B29/B270. We also acknowledge the valuable suggestions made by the referees that help us to improve the manuscript.

Data availability statement

The data that support the findings of this study are available upon reasonable request from the authors.

Declaration of competing interest

The authors declare that they have no known competing financial interests or personal relationships that could have appeared to influence.

Nomenclature

$h_a(j)$	specific enthalpy of humid air at the point j, J kg^{-1}
$h_w(j)$	specific enthalpy of sea water at the point j, J kg^{-1}
$h_b(j)$	specific enthalpy of brine at the point j, J kg^{-1}
$h_{pw}(j)$	specific enthalpy of distillate at the point j, J kg^{-1}
$h_{g_i}(j)$	specific enthalpy of exhaust non-condensable gas i at the point j, J kg^{-1}
$\dot{m}_B$	brine mass flow rate, kg s^{-1}
$\dot{m}_w$	seawater mass flow rate, kg s^{-1}
$\dot{m}_{pw}$	pure water mass flow rate, kg s^{-1}
$\dot{m}_a$	humid air mass flow rate, kg s^{-1}
$\dot{m}_w^E$	flow rate of water in the flue gases, kg s^{-1}
Cp_a	specific heat capacity of air, 1009 J kg^{-1} °C^{-1}
Cp_w	specific heat capacity of liquid water, 4193 J kg^{-1} °C^{-1}
Cp_v	specific heat capacity of water vapor given by (8), J kg^{-1} °C^{-1}
Cp_{g_i}	specific heat capacity of exhaust gases from the seawater heater, J kg^{-1} °C^{-1}
Cp_{N_2}	specific heat capacity of N_2 given by (8), J kg^{-1} °C^{-1}
λ	enthalpy of vaporization of water, 2332.20 kJ kg^{-1}
T	temperature, °C
$x(T)$	absolute humidity of saturated air at the temperature T, non dimensional
$H_{R,j}$	relative humidity of air at point j, %, non dimensional
P	atmospheric pressure, kPa
P_v	vapor pressure, kPa
ϕ	excess of air in the combustion mix, non dimensional
$T^{\oplus}$	standard temperature, 25°C
ϵ_{Rec}	effectiveness of the recuperator, non dimensional
ϵ_B	efficiency of the sea water heater, non dimensional
ϵ_C	effectiveness of the condenser, non dimensional
ϵ_H	effectiveness of the humidifier, non dimensional
$\dot{m}_{air_{ST}}$	mass flow rate of air for stoichiometric mix of H_2 + air, kg s^{-1}
Lc	lower heating value of H_2, 118.680 × 10^6 J kg^{-1}

Abbreviations

HDH	Humidification–dehumidification
NOx	Nitrogen oxides
GOR	Gained output ratio
OCP	Operation cost parameter
NTU	Number of transfer units

ORCID iDs

A Brunini https://orcid.org/0000-0002-6519-5246

A A Melgarejo https://orcid.org/0000-0003-1910-4400

References

[1] El-Dessouky H T and Ettouney H M 2002 *Fundamentals of Salt Water Desalination* (Amsterdam: Elsevier)
[2] Bundschuh J, Kaczmarczyk M, Ghaffour N and Tomaszewska B 2021 State-of-the-art of renewable energy sources used in water desalination: present and future prospects *Desalination* **508** 115035
[3] Qiblawey H M and Banat F 2008 Solar thermal desalination technologies *Desalination* **220** 633–44
[4] Müller-Holst H 2007 Solar thermal desalination using the multiple effect humidification (MEH)-method *Solar Desalination for the 21st Century* (Berlin: Springer) pp 215–25
[5] Kabeel A E, Hamed M H, Omara Z M and Sharshir S W 2013 Water desalination using a humidification–dehumidification technique-a detailed review *Nat. Resour.* **04** 286–305
[6] de Carvalho M D, dos Reis Coimbra J S, Lemos T S M, Bellido J D A and de Oliveira Siqueira A M 2020 A review of humidification–dehumidification desalination systems *Int. J. Res. Granthaalayah* **8** 290–311
[7] de Oliveira Campos B L, da Costa A O S and da Costa Junior E F 2017 Mathematical modeling and sensibility analysis of a solar humidification–dehumidification desalination system considering saturated air *Sol. Energy* **157** 321–7
[8] El-Dessouky H T A 1989 Humidification–dehumidification desalination process using waste heat from a gas turbine *Desalination* **71** 19–33
[9] Attia N F *et al* 2017 The integration of humidification dehumidification desalination and flue gas desulfurization *Desalin. Water Treat.* **60** 48–57
[10] Elnahas M and Ghallab A 2019 Desalination by flue gas humidification–dehumidification using two different flue gas compositions *Mach., Technol., Mater.* **13** 302–5
[11] Dyachenko G and Butov K 2020 Features of simulation of operation of underground hydrogen storage in a cracked porous reservoir *Bull. Eurasian Sci.* **12** 1–13
[12] Dodds P E, Staffell I, Hawkes A D, Li F, Grünewald P, McDowall W and Ekins P 2015 Hydrogen and fuel cell technologies for heating: a review *Int. J. Hydrog. Energy* **40** 2065–83
[13] Peantong S and Tangjitsitcharoen S 2017 A study of using hydrogen gas for steam boilers in chloror–alkali manufacturing *IOP Conf. Ser.: Mater. Sci. Eng.* **215** 12–8
[14] Kalamaras C M and Efstathiou A M 2013 Hydrogen production technologies: current state and future developments *Conf. Papers in Science* vol 213 (Hindawi) pp 27–37
[15] Haeseldonckx D and D'haeseleer W 2007 The use of the natural-gas pipeline infrastructure for hydrogen transport in a changing market structure *Int. J. Hydrog. Energy* **32** 1381–6
[16] Maleki A, Pourfayaz F and Ahmadi M H 2016 Design of a cost-effective wind/photovoltaic/hydrogen energy system for supplying a desalination unit by a heuristic approach *Sol. Energy* **139** 666–75
[17] Jaluria Y 2007 *Design and Optimization of Thermal Systems* (Boca Raton, FL: CRC Press)
[18] Kabeel A E and El-Said E M S 2013 A hybrid solar desalination system of air humidification dehumidification and water flashing evaporation: a comparison among different configurations *Desalination* **330** 79–89
[19] Sharqawy M H, Lienhard J H and Zubair S M 2010 Thermophysical properties of seawater: a review of existing correlations and data *Desalin. Water Treat.* **16** 354–80
[20] Hamed M H, Kabeel A E, Omara Z M and Sharshir S W 2015 Mathematical and experimental investigation of a solar humidification–dehumidification desalination unit *Desalination* **358** 9–17
[21] Hermosillo J-J, Arancibia-Bulnes C A and Estrada C A 2012 Water desalination by air humidification: mathematical model and experimental study *Sol. Energy* **86** 1070–6
[22] Wagner W and Pruß A 2002 The IAPWS formulation 1995 for the thermodynamic properties of ordinary water substance for general and scientific use *J. Phys. Chem. Ref. Data* **31** 387–535
[23] de Oliveira Campos B L, da Costa A O S, de Souza Figueiredo K C and da Costa Junior E F 2018 Performance comparison of different mathematical models in the simulation of a solar desalination by humidification–dehumidification *Desalination* **437** 184–94
[24] Narayan G P, Sharqawy M H, Lienhard V J H and Zubair S M 2010 Thermodynamic analysis of humidification dehumidification desalination cycles *Desalin. Water Treat.* **16** 339–53
[25] Mishra S and Dahiya R P 1989 Adiabatic flame temperature of hydrogen in combination with gaseous fuels *Int. J. Hydrog. Energy* **14** 839–44
[26] Drell I L and Belles F E 1958 *Survey of Hydrogen Combustion Properties* (NACA)
[27] Khanna V, Goel R and Ellzey J 1994 Measurements of emissions and radiation for methane combustion within a porous medium burner *Combust. Sci. Technol.* **99** 133–42
[28] Frassoldati A, Faravelli T and Ranzi E 2006 A wide range modeling study of NO*x* formation and nitrogen chemistry in hydrogen combustion *Int. J. Hydrog. Energy* **31** 2310–28
[29] Chen Q, Finney K, Li H, Zhang X, Zhou J, Sharifi V and Swithenbank J 2012 Condensing boiler applications in the process industry *Appl. Energy* **89** 30–6
[30] Bhatia A 2012 *Improving Energy Efficiency of Boiler Systems* (*Continuing Education and Development Engineering*) (Fairfax, VA: Creative Space Ind. Pub.) pp 1–55
[31] Carpenter K and Kissock J K 2005 *Quantifying Savings from Improved Boiler Operation* (College Station, TX: Texas A & M University)
[32] Mussati S, Manassaldi J I, Benz S J and Scenna N J 2009 Mixed integer nonlinear programming model for the optimal design of fired heaters *Appl. Therm. Eng.* **29** 2194–204
[33] Lowe C, Brancaccio N, Batten D, Leung C and Waibel D 2011 Technology assessment of hydrogen firing of process heaters *Energy Procedia* **4** 1058–65

[34] Bonilla-Petriciolet A, Acosta-Martínez A, Bravo-Sánchez U and Segovia-Hernández J 2006 Bubble and dew point calculations in multicomponent and multireactive mixtures *Chem. Biochem. Eng. Q.* **20** 111–8
[35] Witte L C and Shamsundar N 1983 *A Thermodynamic Efficiency Concept for Heat Exchange Devices* vol 105 (College Station, TX: ASME)
[36] Longoria G, Lynch M and Curtis J 2021 Green hydrogen for heating and its impact on the power system *Int. J. Hydrog. Energy* **46** 26725–40
[37] Lawal D U and Antar M A 2021 Investigation of heat pump-driven humidification–dehumidification desalination system with energy recovery option *J. Therm. Anal. Calorim.* **145** 3177–94
[38] Fouda A, Nada S A, Elattar H F, Rubaiee S and Al-Zahrani A 2018 Performance analysis of proposed solar HDH water desalination systems for hot and humid climate cities *Appl. Therm. Eng.* **144** 81–95
[39] Amara M B, Houcine I, Guizani A and Mâalej M 2004 Experimental study of a multiple-effect humidification solar desalination technique *Desalination* **170** 209–21
[40] Habeebullah B *et al* 2010 Performance analysis of a combined heat pump-dehumidifying system *J. King Abdulaziz Univ. Eng. Sci.* **21** 97–114
[41] He W F, Chen J J, Zhen M R and Han D 2019 Thermodynamic, economic analysis and optimization of a heat pump driven desalination system with open-air humidification dehumidification configurations *Energy* **174** 768–78
[42] He W, Yang H and Han D 2019 Thermodynamic investigation and optimization of a heat pump coupled open-air, open-water humidification dehumidification desalination system with a direct contact dehumidifier *Desalination* **469** 114101
[43] He W F, Han D and Ji C 2018 Investigation on humidification dehumidification desalination system coupled with heat pump *Desalination* **436** 152–60
[44] He W F, Wen T, Han D, Luo L T, Li R Y and Zhong W C 2019 Energetic, entropic and economic analysis of a heat pump coupled humidification dehumidification desalination system using a packed bed dehumidifier *Energy Convers. Manage.* **194** 11–21
[45] Dehghani S, Date A and Akbarzadeh A 2018 Performance analysis of a heat pump driven humidification–dehumidification desalination system *Desalination* **445** 95–104
[46] Zhang Y, Zhu C, Zhang H, Zheng W, You S and Zhen Y 2018 Experimental study of a humidification–dehumidification desalination system with heat pump unit *Desalination* **442** 108–17
[47] Shafii M B, Jafargholi H and Faegh M 2018 Experimental investigation of heat recovery in a humidification–dehumidification desalination system via a heat pump *Desalination* **437** 81–8
[48] Faegh M and Shafii M B 2019 Performance evaluation of a novel compact humidification–dehumidification desalination system coupled with a heat pump for design and off-design conditions *Energy Convers. Manage.* **194** 160–72
[49] Lawal D U, Zubair S M and Antar M A 2018 Exergo-economic analysis of humidification–dehumidification (HDH) desalination systems driven by heat pump (HP) *Desalination* **443** 11–25
[50] Rostamzadeh H, Namin A S, Ghaebi H and Amidpour M 2018 Performance assessment and optimization of a humidification dehumidification (HDH) system driven by absorption-compression heat pump cycle *Desalination* **447** 84–101
[51] Santosh R, Kumaresan G, Kumar G K and Velraj R 2020 Experimental parametric investigation of waste heat powered humidification dehumidification system for production of freshwater from wastewater *Desalination* **484** 114422
[52] Giwa A, Fath H and Hasan S W 2016 Humidification–dehumidification desalination process driven by photovoltaic thermal energy recovery (PV-HDH) for small-scale sustainable water and power production *Desalination* **377** 163–71
[53] Zhani K 2013 Solar desalination based on multiple effect humidification process: thermal performance and experimental validation *Renewable Sustainable Energy Rev.* **24** 406–17
[54] Dehghani S, Date A and Akbarzadeh A 2019 An experimental study of brine recirculation in humidification–dehumidification desalination of seawater *Case Studies in Thermal Engineering* **14** 100–463
[55] Lattemann S and Höpner T 2008 Environmental impact and impact assessment of seawater desalination *Desalination* **220** 1–15
[56] Chafik E 2003 A new seawater desalination process using solar energy *Desalination* **153** 25–37